# Truncation and Optimisation of Peptide Inhibitors of Cyclin-Dependent Kinase 2-Cyclin A Through Structure-Guided Design

**ARTICLE** *in* CHEMMEDCHEM · JUNE 2009

Impact Factor: 2.97 · DOI: 10.1002/cmdc.200900093 · Source: PubMed



**8 AUTHORS**, INCLUDING:

George Kontopidis
University of Thessaly
**77** PUBLICATIONS **1,725** CITATIONS
SEE PROFILE

Martin J I Andrews
Galapagos NV
**27** PUBLICATIONS **373** CITATIONS
SEE PROFILE

Campbell Mcinnes
University of South Carolina
**109** PUBLICATIONS **1,979** CITATIONS
SEE PROFILE

Peter Fischer
University of Nottingham
**289** PUBLICATIONS **4,326** CITATIONS
SEE PROFILE

DOI: 10.1002/cmdc.200900093

# Truncation and Optimisation of Peptide Inhibitors of Cyclin-Dependent Kinase 2-Cyclin A Through Structure-Guided Design

George Kontopidis,[a] Martin J. Andrews,[b] Campbell McInnes,[c] Andy Plater,[d] Lorraine Innes,[d] Scott Renachowski,[d] Angela Cowan,[d] and Peter M. Fischer*[e]

The cyclin-dependent kinase 2–cyclin A complex is an important regulator of the DNA-synthesis phase of the mammalian cell cycle, which is frequently deregulated in cancer. Rather than blocking the ATP-binding site of the apparently redundant kinase subunit, targeting the binding site for macromolecular substrates and regulatory proteins of cyclin A represents a promising strategy to enforce tumour-selective apoptosis. The cyclin-binding groove can be blocked with comparatively small synthetic peptides, which indirectly leads to inhibition of kinase function, but these peptides are metabolically labile and membrane impermeable. As part of our ongoing effort to develop more druglike peptidomimetics derived from cyclin-groove-binding peptides, we report the results of our studies aimed at a detailed understanding of the structural determinants required for effective binding. Using a combination of peptide synthesis, biochemical assays and X-ray crystallography, we show that it is possible to simplify peptide structures through the replacement of dipeptide units in which one of the residues is not directly involved in binding, through the introduction of β-amino acid residues that retain only the dipeptide residue side chain that is important for binding. This approach also allowed us to probe spatial constraints in general, as well as the importance of peptide backbone hydrogen-bonding functions. Our identification of potent β-homoleucine-containing tetrapeptide inhibitors, as well as the finding that an optimised N-terminally acetylated tripeptide retains some cyclin A-binding affinity, suggest that the pharmacological targeting of the cyclin A binding groove may be feasible.

## Introduction

The system of checkpoints that controls normal cellular replication is termed the cell cycle, but in cancer cells these checkpoints often become deregulated and cell proliferation occurs in an uncontrolled fashion. The kinase complex CDK2–cyclin A (CDK2A) operates primarily in the DNA synthesis phase (S phase) of the cell cycle, ensuring the replication of a single copy of DNA.[1] Cyclin A, the activator subunit of CDK2 in the CDK2A complex, is expressed at the beginning of S phase and is then degraded as the cell passes through the second gap phase (G2) and into mitosis. CDK2A controls the activities of both transcriptional repressors (e.g. retinoblastoma (Rb) family proteins) and promoters (e.g. E2F family transcription factors).[2] Initially, the CDK2A complex maintains Rb hyperphosphorylation at the beginning of S phase, thus dissociating Rb–E2F complexes and activating E2F. This is followed by CDK2A-mediated phosphorylation of E2F at the end of S phase, terminating E2F transcriptional activity. It has been recognised and validated that pharmacological inhibition of CDK2A leads to inappropriate persistence of E2F activity after completion of S phase, which results in E2F-induced apoptosis.[3,4] Cells with constitutively deregulated E2F activity—that is, most cancer cells—are especially sensitive to this inhibition, and CDK2A inhibition therefore represents a promising tumour-selective therapeutic strategy.[5] Small-molecule ATP-antagonist CDK inhibitors are being developed, at least partly, based on this hypothesis.[6,7] However, this approach remains difficult, especially because highly selective inhibitors of kinase ATP-binding sites are elusive, and cyclin A-associated kinase activity appears to be functionally redundant.[7]

Phosphorylation of CDK2A substrates such as the Rb proteins requires an initial recognition step that involves the so-called cyclin binding groove (CBG) of cyclin A,[8] which is structurally different to the CBG in other cyclins.[9,10] CDK2A activity is also regulated by tumour suppressor CDK inhibitor (CDKI) proteins, such as $p21^{WAF1/CIP1}$ and $p27^{KIP1}$, which block both the kinase catalytic site, as well as the CBG.[11] These CDKIs and CDK2A substrates share a cyclin-binding motif (CBM), with the sequence zRxLyy′, where z and x are basic residues, y is a hydrophobic residue, and y′ is Gly or a hydrophobic residue.[8] We and others have characterised the CBM and CBG extensive-

[a] Dr. G. Kontopidis[+]
Veterinary School, University of Thessaly, Karditsa 43100 (Greece)
[b] Dr. M. J. Andrews[+]
Galapagos NV, Generaal De Wittelaan L11A3, 2800 Mechelen (Belgium)
[c] Dr. C. McInnes[+]
South Carolina College of Pharmacy, University of South Carolina
Columbia, SC 29208 (USA)
[d] Dr. A. Plater, L. Innes, Dr. S. Renachowski, A. Cowan
Cyclacel Ltd., James Lindsay Place, Dundee DD1 5JJ (UK)
[e] Prof. P. M. Fischer
School of Pharmacy and Centre for Biomolecular Sciences
University of Nottingham, University Park, Nottingham NG7 2RD (UK)
Fax: (+44) 115-951-3412
E-mail: peter.fischer@nottinham.ac.uk
[+] These authors contributed equally to this work

   

ly through X-ray crystallography studies,[10–15] and this has provided a foundation for the design of synthetic peptides as indirect inhibitors of CDK2A kinase activity.[4,16–19] Analysis of appropriate crystal structures and peptide mapping studies have shown that certain p21-derived octapeptides, which formed the starting point for the studies reported here (Figure 1a),

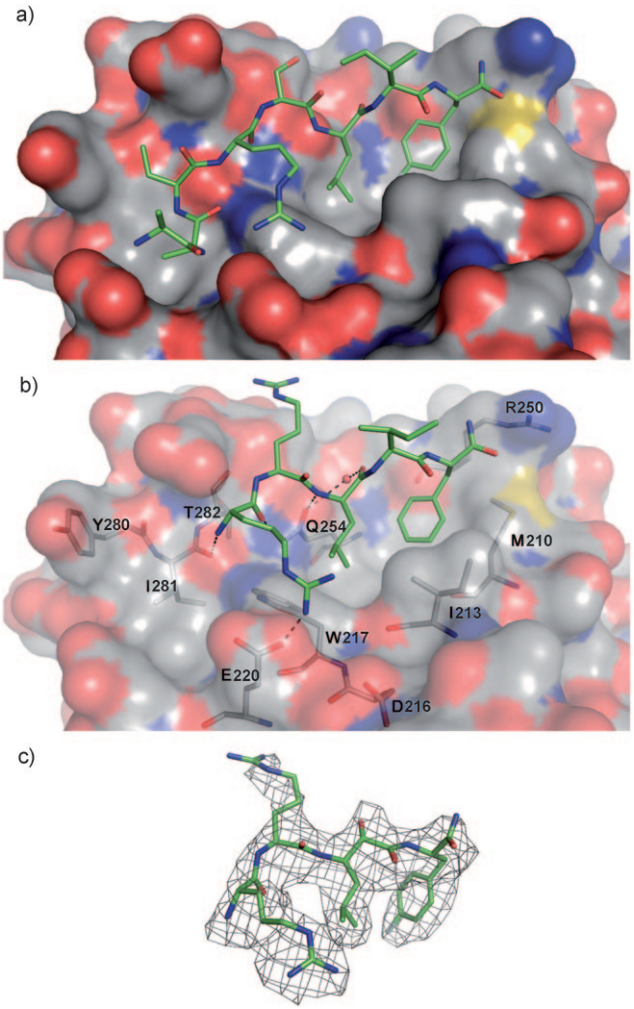


**Figure 1.** a) Binding pose of optimised octamer CBM peptide (H-AlaAlaAbu-ArgSerLeuIlePhe-$NH_2$; green CPK stick model) in the CBG (gray CPK surface; constructed from PDB: 2C5V[21]). b) Binding of a CBM pentapeptide (H-Arg-ArgLeuIlePhe-$NH_2$) to the CBG (intermolecular H bonds are shown as broken lines; key residues in the CBG are shown as grey sticks and are labelled; constructed from PDB: 1OKV[14]) c) Example electron density difference map for one of the peptide ligands (**21**) in the CDK2A complex crystal structures determined in this study (shown as a mesh at 1.5 σ level).

represent an optimal form of the CBM.[8,14] Although CBM peptides can be equipped with cell delivery vectors[20] in order to be able to reach their intracellular target when applied extracellularly in vitro[8] and even in vivo,[4] it remains to be seen if such peptide constructs can be developed as drugs. We have therefore embarked on a programme of peptidomimetic redesign of CBM peptides with the ultimate goal of developing potent, cell-permeable, and generally druglike CBG inhibitors.

In a first step towards this goal we have recently described the identification of nonpeptide surrogates for the termini of the CBM in the context of peptide hybrids.[16] This stimulated us to investigate more closely whether replacement of other groups in the peptide lead sequences was possible. Analysis of CBM peptide–CDK2A complex structures shows that certain CBM residues act as spacers, since their side chains do not directly participate in binding and are tolerant of substitution (Figure 1). It should therefore be possible to remove these residues, provided the overall structural and conformational constraints necessary for productive binding can be maintained. Appropriate positioning of the lipophilic Leu and Phe side chains (where Phe corresponds to y or y′ in zRxLyy′) in the hydrophobic subpocket of the CBG is especially important in this respect. In this context it is already known that the presence of a spacer residue between the Leu and Phe residues increases complementarity and results in higher affinity. For example, p27-derived peptides contain a LeuPheGly (Lyy′) terminus and show lower affinity compared to p21-derived peptides with the LeuIlePhe terminus, despite the fact that the Ile side chain in the latter does not make any contacts with the CBG.[22] One method of altering the spacing of side chains in peptides is by incorporation of β-amino acids, which differ from the normal proteinaceous α-amino acids by the extension of the backbone with a methylene group. We therefore hypothesised that substitution of β-homoLeu for Leu in the p27 context (LeuPheGly) would improve complementarity and allow p21-like interactions (LeuIlePhe). In addition, substitution of β-residues in other positions was predicted to generate useful structure–activity relationship (SAR) information to establish further structural determinants of CBG inhibition.

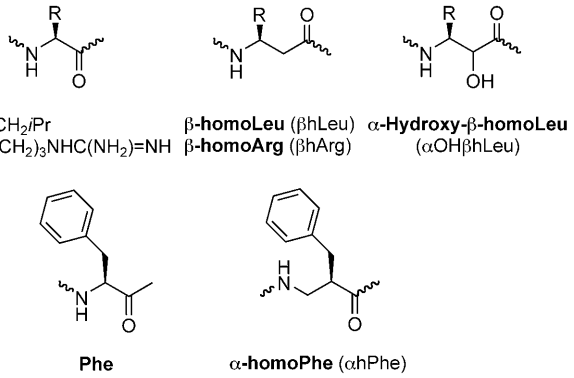


The chemical structures of β-amino acids present an additional level of complexity over α-amino acids as the side chain can be attached at either the α- or β-carbon atom. The incorporation into peptides of either form will result in different positioning of the backbone amide bonds in the peptides. As an additional probe of peptide backbone binding determinants, α-hydroxy-β-amino acids were incorporated as these include a functionality that could potentially reproduce the backbone H-bonding arrangements of native peptides. Using these and other residue replacement strategies, we have established SARs that enabled identification of a minimal CBG inhibitory peptide.

  

## Results and Discussion

### SAR for spacing of CBM residues interacting with the CBG hydrophobic pocket

Peptide SAR studies of the CBM determinants of binding to the main hydrophobic pocket of the CBG have previously been reported, where the optimal motif contains a LyF sequence.[8] In our previously published[14,17,22] details of the binding modes of octa- (Figure 1a) and pentapeptides (Figure 1b) with CDK2A, neither intra- nor intermolecular interactions of Ile (residue y, Ile158 in p21 numbering) were observed, with this position being largely tolerant to substitution. These observations were reinforced by considering the biological activity of peptides containing different residues between Leu and Phe (Table 1 and Table 2). This pattern was observed with a number of other amino acid mutations of the p21 sequence (data not shown),[8,22] suggesting the role of the spacer residue y is mainly structural, providing the correct orientation of the interacting Leu and Phe residues. Apart from the hydrophobic interactions of the Leu and Phe side chains, the ionic interaction of the Arg (Arg in zRxLyy′; Arg155 of p21) guanidine group also plays a critical role in CBG recognition. A spacing function similar to that of the Ile residue discussed above has also been observed with a neighbouring Arg residue (in p21 x of zRxLyy′ is also Arg; Figure 1b), where a number of potential substitutions are tolerated, including the incorporation of side chain-to-head cyclic amide groups.[17]

**Table 1.** Cyclin A binding and CDK2A kinase inhibition potency of octapeptides **1**–**7**.[a]

| No. | Sequence | CDK2A $IC_{50}$ [μM] Binding | Kinase |
|---|---|---|---|
| **1** | H-HisAlaLysArgArgLeuIlePhe-$NH_2$ | 0.05 | 0.14 |
| **2** | H-AlaAlaAbuArgArgLeuIle*p*FPheNH$_2$ | 0.002 | 0.08 |
| **3** | H-AlaAlaAbuArgArgLeuPhe-$NH_2$ | 0.14 | 1.9 |
| **4** | H-AlaAlaAbuArgArgβhLeuPhe-$NH_2$ | 0.07 | 0.30 |
| **5** | H-AlaAlaAbuArgArgLeuαhPhe-$NH_2$ | 12.9 | 158 |
| **6** | H-AlaAlaAbuArgArgβhLeuαhPhe-$NH_2$ | >100 | >100 |
| **7** | H-AlaAlaAbuβhArgβhLeuPhe-$NH_2$ | >100 | >100 |

[a] Values are reported as the mean of at least two independent determinations; abbreviations: Abu, 2-aminobutyric acid; *p*FPhe, *para*-fluorophenylalanine; βhArg, β-homoarginine; βhLeu, β-homoleucine; αhPhe, α-homophenylalanine.

The substitution of β-amino acids into the CBM offers the possibility further to examine the optimal spacing between the Leu and Phe residues, while reducing overall peptide mass and simplifying the sequence. In the context of the octapeptides **1**–**3**, the main CBG-interacting residues were therefore probed through introduction of β-residues (Table 1) to determine the most effective positioning of binding determinants and to examine the contributions of backbone H bonds to overall affinity. Initially, we sought to correlate the activity of the peptides with the proximity between the Leu and Phe side chains by increasing the intervening distance incrementally. Peptide **3** contains a p27-like C-terminal hydrophobic motif (LeuPheGly), but lacks the Gly residue, and thus represents the shortest possible distance between these side chains. This peptide showed good activity, and although it was an effective reference point, was still considerably less active than the lead peptides **1** and **2**. Incorporation of β-homoLeu in this context to generate peptide **4** was favourable for binding and functional activity, and in fact resulted in increased potency with respect to **3**, therefore more closely approximating the positioning of the two hydrophobic residues as in the p21 arrangement. Comparing the kinase inhibition of the corresponding peptides, replacement of Leu in **3** with β-homoLeu as in **4** resulted in a 6-fold activity increase.

**Table 2.** Cyclin A binding and CDK2A kinase inhibition potency of peptides **8**–**23**.[a]

| No. | Sequence | CDK2A $IC_{50}$ [μM] Binding | Kinase |
|---|---|---|---|
| **8** | H-ArgArgLeuIlePhe-$NH_2$ | 1.06 | 11.2 |
| **9** | H-ArgArgβhLeuPhe-$NH_2$ | 1.80 | 1.77 |
| **10** | Ac-ArgArgLeuIlePhe-$NH_2$ | 12.7 | 26.7 |
| **11** | Ac-ArgArgβhLeuPhe-$NH_2$ | 34 | 238 |
| **12** | Ac-ArgArgβhLeuMePhe-$NH_2$ | 30 | >250 |
| **13** | H-ArgArgLeuAsn*p*FPhe-$NH_2$ | 0.54 | 6.3 |
| **14** | H-ArgArgβhLeu*p*FPhe-$NH_2$ | 0.33 | 1.03 |
| **15** | H-ArgArgβhLeu*m*FPhe-$NH_2$ | 0.46 | 2.67 |
| **16** | H-ArgArgβhLeu*m*ClPhe-$NH_2$ | 0.54 | 2.65 |
| **17** | Ac-ArgArgLeuAsn*p*FPhe-$NH_2$ | 6.66 | 11.9 |
| **18** | Ac-LeuAsn*p*FPhe-$NH_2$ | 55 | 139 |
| **19** | Ac-βhLeu*p*FPhe-$NH_2$ | >250 | >250 |
| **20**[b] | H-ArgArgαOHβhLeu*p*FPhe-$NH_2$ | 1.58 | 15.5 |
| **21**[b] | H-ArgArgαOHβhLeu*p*FPhe-$NH_2$ | 3.95 | 6.83 |
| **22**[b] | H-CitCitαOHβhLeu*p*FPhe-$NH_2$ | >100 | >100 |
| **23**[b] | H-CitCitαOHβhLeu*p*FPhe-$NH_2$ | 14.2 | >100 |

[a] Values are reported as the mean of at least two independent determinations; abbreviations: Abu, 2-aminobutyric acid; Cit, citrulline; *p*FPhe, *para*-fluoro-phenylalanine; *m*FPhe, *meta*-fluoro-phenylalanine; mClPhe, *meta*-chloro-phenylalanine; βhArg, β-homoarginine; βhLeu, β-homoleucine; αhPhe, α-homophenylalanine; αOHβhLeu, α-hydroxy-β-homoleucine. [b] By inference from the peptide **21**–CDK2A complex X-ray crystal structure, **21** contains α-hydroxy-β-homoleucine with the *R* configuration at $C^{\alpha}$, whereas **20** is the *S*-epimer; assuming the same RP-HPLC elution order of the epimer pairs for **20**–**21** and **22**–**23**, the latter likely correspond to the *S*- and *R*-epimers, respectively, of the Cit peptides.

Corresponding replacements were also made in three instances in the context of penta- (Leu) and tetrapeptide (β-homoLeu) sequences (Table 2). The results show that the benefit provided by the β-homoLeu modification was context-dependent. The relative potency of **10** and **11** showed a twofold decrease, whereas comparing **8** with **9** indicated less than twofold decrease in activity. In the context of the *para*-fluoro-substituted Phe (*p*-F-Phe) derivative pair **13** and **14**, the β-homoLeu analogue actually possessed increased activity (1.6-fold) relative to the p21-like motif, suggesting that perhaps the conformational adaptability of the β-homoLeu residue allows more optimal interactions of the fluorinated Phenyl ring with the lipophilic CBG pocket. From these results, although recovery of activity relative to the p27-like sequence was obtained, it is apparent that in comparison to the p21 LyF motif, dele-

  

tion of the spacer and incorporation of β-homoLeu resulted in slightly less potent inhibitors and incomplete recovery when the peptides bound weakly. For tighter-binding peptides ($IC_{50}$ $<1$ μM), the incorporation of β-homoLeu resulted in potency increase.

The incorporation of β-amino acids introduces a structurally flexible methylene bridge that is better tolerated in the more potent sequence contexts, which anchor tightly to the CBG (Table 1 and Table 2). The p21 (LeullePhe) arrangement is known to be more active than the corresponding p27 motif (LeuPheGly) and increasing the spacing between the side chains with the use of β-homoLeu to mimic this is sufficient to counteract the additional rotatable bonds and resulting entropic binding cost. However, this was less tolerated in peptides with medium, weak, and very weak activity (**8**–**11**, **18**, **19**) than in the more potent peptide pairs (**13**, **14**).

In order to determine the structural basis for the potency changes observed upon introduction of β-homoLeu, the X-ray crystal structure of compound **11** bound to CDK2A was determined to a resolution of 2.4 Å (Figure 2a, Table 3). Alignment of the peptide-binding pose with those of the LeullePhe (y and y′ in Lyy′ corresponding to Ile and Phe) containing peptide **8** and a cyclic peptide[17] containing the LeuPheGly (y and y′ in Lyy′ corresponding to Phe and Gly) indicated that the decrease in affinity resulted from less optimal interactions of the Leu side chain (Figure 1b and Figure 3). The β-homoLeu analogue had approximately half of the total van der Waals contacts observed with the native p21 LeullePhe sequence. As the Phe residue makes similar contacts in both contexts, comparison of the structures indicates that these interactions are preserved at the expense of less optimal Leu interactions. The conclusion can be drawn that the conformational preferences of the β-homoLeu tetrapeptide prohibit full complementarity of this motif with the hydrophobic CBG pocket.

In order to explore spacing geometry further, substitution of the Phe residue with a β-amino acid was carried out, both singly and in combination with β-homoLeu. Based on modelling studies, the β-Phe residue used was α-homoPhe—that is, the Phe homologue with the side chain on the α-C as opposed to β-homoLeu, where the side chain is on the β-C. For the single substitution, peptide **5** displayed much lower activity compared to the parent p21 peptide and to the individual β-homoLeu substitution peptides. This indicates that while the spacing and number of rotatable bonds in this context was similar to the β-homoLeu substitution, the geometric preferences of the α-homoPhe residue did not allow favourable enthalpy of binding. Further incorporation of both non-natural residues in **6** resulted in a very flexible linker, and somewhat surprisingly, this peptide showed no appreciable activity. This is noteworthy, as the arrangement has a spacing closest to the p21 motif (peptide **1**), but possesses an increased number of rotatable bonds. As a whole, these results suggest that the entropic cost of reaching a binding conformation had a deleterious effect when the two β-amino acids were incorporated simultaneously.

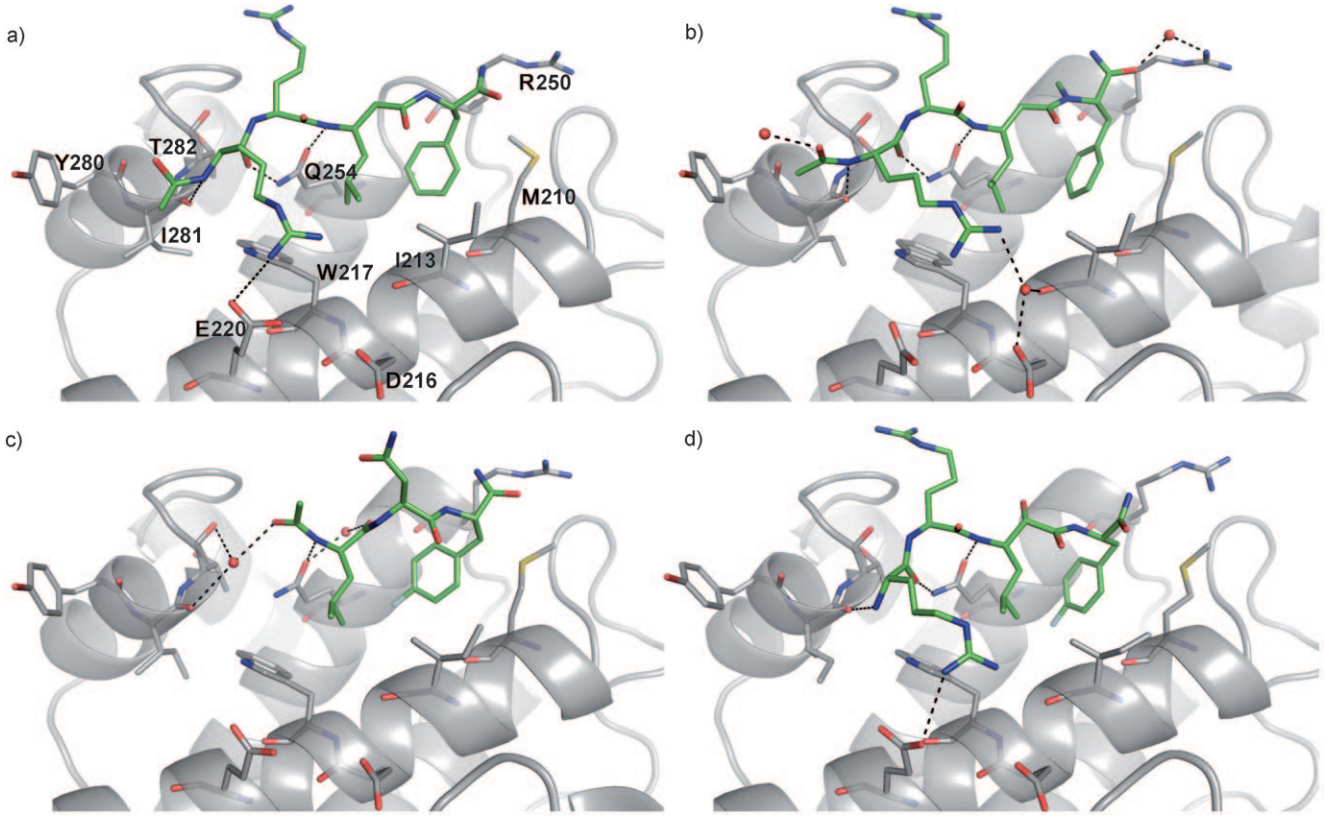


**Figure 2.** Cyclin A binding modes of peptides a) **11**, b) **12**, c) **18**, and d) **21**. The CBG is depicted as a secondary structure cartoon, with key residues as stick models (gray CPK; labelled in Figure 2a), the ligands as green CPK stick models. H bonds are shown as broken lines.

  

**Table 3.** X-Ray crystallography data for CDK2A complexes with peptides **11**, **12**, **18**, and **21**.

| Data collection | Peptide | | | |
|---|---|---|---|---|
| | **11** | **12** | **18** | **21** |
| Space group | $P2_12_12_1$ | $P2_12_12_1$ | $P2_12_12_1$ | $P2_12_12_1$ |
| Unit cell *a* (Å) | 74.7 | 74.5 | 74.6 | 74.4 |
| *b* (Å) | 115.9 | 113.8 | 114.3 | 114.9 |
| *c* (Å) | 158.1 | 158.5 | 154.3 | 154.5 |
| Max. resolution (Å) | 2.4 | 2.3 | 2.75 | 2.9 |
| Observations | 628,198 | 251,155 | 125,501 | 92,674 |
| Unique reflections | 46,387 | 62,221 | 33,628 | 30,103 |
| Completeness (%) | 95 | 96.4 | 98.3 | 98 |
| $R_{merge}$[1] | 0.09 | 0.094 | 0.14 | 0.12 |
| Mean I/σ | 6.69 | 15.5 | 12.7 | 10.5 |
| Highest resolution bin (Å) | 2.56-2.53 | 2.42-2.3 | 2.9–2.75 | 3.06-2.9 |
| Mean I/σ (highest resolution bin) | 1.34 | 1.8 | 1.9 | 1.6 |
| $R_{merge}$[1] (highest resolution bin) | 0.3 | 0.28 | 0.68 | 0.67 |
| *Refinement* | | | | |
| Protein atoms | 8754 | 8932 | 8924 | 8932 |
| Inhibitor atoms | 46 | 47 | 32 | 45 |
| Water molecules | 554 | 656 | 133 | 183 |
| Reflections used in refinement | 41,834 | 55,318 | 33,624 | 28,324 |
| $R_{factor}$ | 19.3 | 18.7 | 19.5 | 18.9 |
| $R_{free}$ | 25.9 | 24.2 | 25.7 | 25.2 |
| Mean B-factor protein (Å$^2$) | 51.7 | 22.3 | 46.3 | 58.8 |
| Mean B-factor ligands (Å$^2$) | 63.2 | 28.4 | 69.4 (52%) | 83.4 (42%) |
| Mean B-factor, solvent (Å$^2$) | 55.4 | 29.0 | 43.8 | 60.2 |

We next sought to determine whether substitution of the aromatic ring of the Phe residue (Phe 159 in p21 numbering) in the β-peptide series would give SAR patterns consistent with those previously established in the p21 and p27 contexts.[8,14,17] In the p21 case, peptides with the Phe aromatic ring *para*-substituted with halogens were the most active, whereas the conformational requirements attendant upon binding of the p27 LeuPheGly motif favoured *meta*-substituted Phe peptides. Here Phe modifications were carried out in the context of the tetrapeptide containing β-homoLeu and showed that the *para*-fluoro derivative **14** bound slightly better (compare peptides **13**–**16**). These results suggest that the greater flexibility imparted by the β-amino acid methylene bridge allowed increased tolerance of different Phe substitutions, and that the optimal p21 modification was the most favourable one in this case.

### Further SAR studies on the conformational determinants of CBG inhibition

In addition to modification of the hydrophobic pocket interactions, attempts were also made to modify the charged anchor of the p21 sequence. Optimised pentapeptides that contain two consecutive Arg residues (Arg 1 and Arg 2 corresponding to R and x, respectively, in zRxLyy′; Arg 155 and Arg 156 of p21) have been reported previously.[8] While Arg 1 is highly resistant to modification and replacement, the less critical Arg 2 can be replaced with nonconservative residues without significantly compromising affinity. Since Arg 2 appears to play more of a spacing function than Arg 1, we tested the incorporation of β-homoArg as an Arg 1,2 substitution, to generate compound **7**, within the active β-homoLeu arrangement. Since this peptide was found to be inactive, the suggestion is that the crystallographically observed backbone H bonds in H-ArgArg-LeuIlePhe-$NH_2$ from Arg 2 were essential for activity (Figure 1b).

As discussed above, the role of the Ile residue in the p21 LeuIlePhe context has been suggested to be mainly structural. Some differences have been observed between activity results for peptides containing the bulky Ile (more active) and short Ala (less active) side chains, an indication of the dependence on structural flexibility in this position.[8] Based on this observation, we sought to modify the linkage between the Leu and Phe residues to reduce flexibility further and perhaps decrease the entropic cost of binding. Incorporation of a methyl group onto the Phe amide nitrogen to generate peptide **12** produced comparable activity to **11**, suggesting that the conformational preferences are similar in both cases. Further insights were obtained by examining the crystal structure of the N-methylated peptide **12** bound to CDK2A (Figure 2b). Unexpectedly, this showed that the conformation of the Leu and Phe backbone and side chains deviated significantly from that observed for corresponding complexes of **11** and similar peptides. This suggests that the β-homoLeu scaffold is quite tolerant to modification, preserving activity, a result that is potentially important in inhibitor development since the methylated amide bond will be more resistant to proteolysis.

We had previously determined that truncation of an octamer series to pentameric peptides was possible with retention of considerable activity,[8] so this approach was attempted in the β-peptide series. As can be seen, **11** retained considerable activity, although the terminally nonacetylated form **9** showed superior activity. This effect had been noted previously, and reinforces the importance of the peptide backbone H bonds in the N-terminal region. The crystal structure of **11** bound to CDK2A (Figure 2a) indicates that acetylation increased the H-bond distance of the N terminus to the backbone carbonyl group of Ile 281 to 3.3 Å (weak H bond) from 2.9 Å (strong H bond) for the protonated amine of **9**.

### Backbone modifications and determination of minimised CBM

Despite the retention of considerable activity in the β-peptide series, incorporation of β-homoLeu eliminates a potentially energetically favourable H-bond network formed from Gln 254 in

  

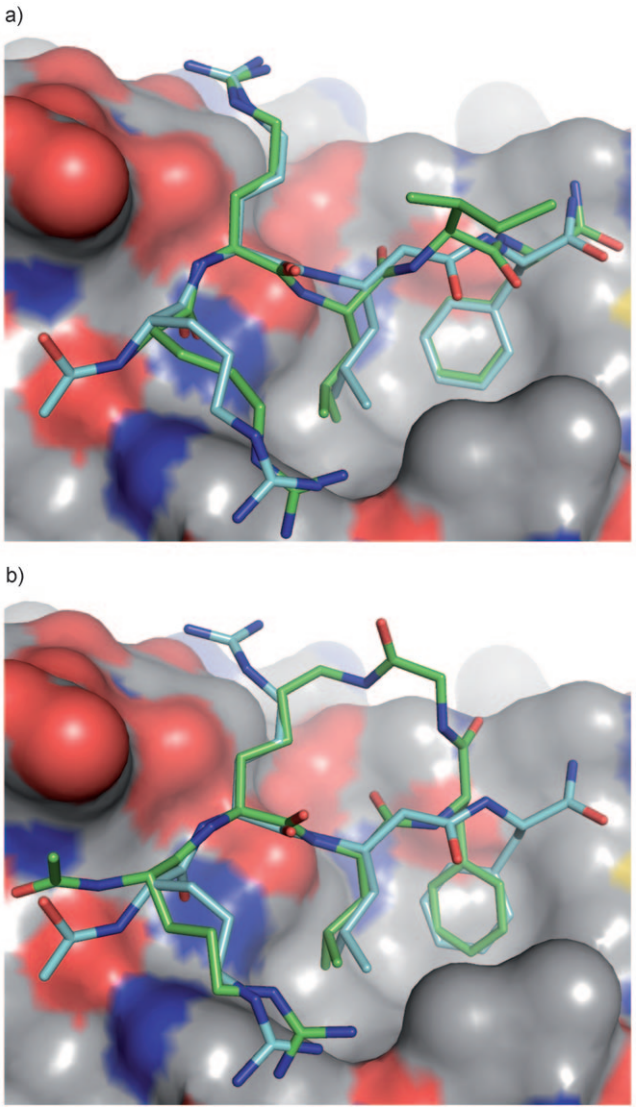


**Figure 3.** Alignment of the X-ray crystal structures of the CDK2A complex of β-peptide **11** with a) that of peptide **8** (PDB: 1OKV[14]), and b) that of a p27 LFG motif-containing side chain-to-tail cyclic peptide Ac-ArgLysLeuPheGly (PDB: 1URC[17]). The CBG is depicted as a gray CPK surface, peptide **11** is shown as a cyan CPK stick model, whereas peptide **8** and the cyclic peptide are shown as green CPK stick models.

the CBG through a water molecule to the carbonyl oxygen of the LyF Leu backbone (Figure 1b). Reintroduction of this bridged H bond could therefore potentially contribute to the binding energy. To test this idea we incorporated an α-hydroxy-β-homoLeu residue to generate peptides **20** and **21**. These Leu replacements were deemed appropriate as they contain a hydroxy group at a position potentially suitable to act as an H-bond acceptor similar to the carbonyl group of Leu in peptides not containing β-residues. The $N^{\alpha}$-Fmoc-protected form of α-hydroxy-β-homoLeu [(2*R*/*S*,3*S*)-3-amino-2-hydroxy-5-methylhexanoic acid] required for peptide synthesis was prepared as shown in Scheme 1, starting from $N^{\alpha}$-*Z*-L-Leu-OH, which was converted to the corresponding amino aldehyde via lithium aluminium hydride reduction of the *N*-methoxy-*N*-methylcarboxamide derivative,[23] followed directly by addition

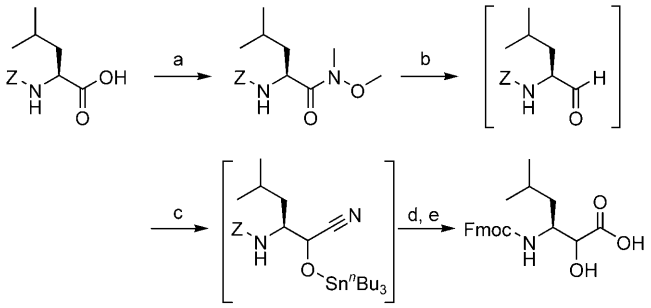


**Scheme 1.** Synthesis of Fmoc-α-hydroxy-β-homoleucine. *Reagents and conditions*: a) WSC, HNMe(OMe), *i*Pr$_2$NEt, $CH_2Cl_2$, RT, 2 h; b) $LiAlH_4$, THF, RT, 10 min; c) *n*Bu$_3$SnCN, $CH_2Cl_2$, −40 °C, 30 min; d) aq HCl/dioxane (1:1), Δ, 12 h; e) Fmoc-ONSu, aq $NaHCO_3$, RT, 12 h; overall yield 12%.

to the aldehyde of tributyltin cyanide to form the tributylstannyl cyanohydrin,[24] which was hydrolysed and $N^{\alpha}$-Fmoc protected.[25] After assembly by standard methods, the peptide epimers were separated by preparative RP-HPLC. Although both peptide epimers retained activity, they were considerably less potent than the reference β-homoLeu peptide **14**. Isomers **20** and **21** were about five- and tenfold lower in activity, respectively. Previously, the incorporation of citrulline (Cit; an Arg isostere where the guanidine group is replaced with an uncharged urea group) into the p21-derived peptides was shown to retain significant activity.[8] Synthesis of the generally less active CitCit compounds (**22** and **23**) was therefore also undertaken, and comparison of these results showed only **23** to be marginally active in the binding assay.

Overall, it is possible that the general decrease in activity in the α-hydroxy-β-homoLeu series was due to the additional conformational restraint imposed by the hydroxy group, which could preclude the optimal bioactive configuration. To determine the structural basis for the potency decrease, a crystallographic study was performed to determine if the hydroxy group participated in H bonding. A CDK2A complex crystal structure of the peptide α-hydroxy-β-homoLeu epimer with the *R*-carbinol stereochemistry (**21**) was solved and showed that the hydroxy group (Figure 2d) occupied the same position as the Leu backbone carbonyl group in peptides containing Leu (Figure 1a and b) and therefore should be able to form a water-mediated H bond with the carbonyl oxygen of Gln 254. As the resolution of this structure was 2.9 Å (Table 3), the presence of a bridging water molecule could not be confirmed unambiguously and therefore it is not possible to determine from these data if introduction of the hydroxy group did in fact re-establish a favourable water-mediated H bond. Superposition of crystal structures of **11** and **21** revealed that a shift occurred only in the region of the Phe amide nitrogen and that overall the hydrophobic determinants of the hydroxylated β-homoLeu occupy similar positions to the unsubstituted derivative. This suggests that the hydroxylated peptide has an unfavourable internal energy relative to the other analogues.

As a result of the SAR and crystallographic information described above, which indicates that optimised truncated peptides could be obtained, we sought to determine the minimal

  

active pharmacophore of the CBM. Previously, results had shown that truncation of p21 peptides below pentamers resulted in loss of detectable activity.[8] The requirement for peptide backbone H bonding around Arg 2 suggested that incorporation of appropriate functionality might allow structural simplification. We hypothesised that acetylation might achieve mimicry of the amide interactions and therefore the hydrophobic tripeptide **18** was synthesised. Remarkably, this compound was found to show low, but appreciable, activity, thus validating the hypothesis. Crystallographic study of the complex of **18** with CDK2A (Figure 2c) indicated that the tripeptide bound in a very similar mode to other p21 motif peptides. The weak affinity of this complex is reflected in the highest observed difference in temperature factors between protein and peptide in this case compared to all other peptide–CDK2A structures (Table 3). A key contribution of the N-terminal acetyl group to binding is a *cis* arrangement of the amide bond, thus maintaining the observed amide nitrogen H bond to Gln 524 and also allowing formation of an additional H bond with Thr 282 of cyclin A through a water molecule (Figure 2c). The observation of this interaction provides further insight into determinants of CBG inhibition and provides input for the design of nonpeptide inhibitors. Finally, in order further to examine the contributions of the hydrophobic motif to binding, we synthesised the acetylated dipeptide version of **18**, incorporating β-homoLeu (**19**). However, this analogue showed no detectable activity.

## Conclusions

We have synthesised, tested, and structurally characterised a number of CBM peptides. The results obtained provide insights into the determinants for optimal spacing of the key hydrophobic residues, into the contributions of H-bonding groups, and additionally into defining the minimal pharmacophore for CBG inhibition. Overall, it has been demonstrated that in tightly-bound inhibitors, incorporation of β-homoLeu can be used to simplify the structure and peptidic character of inhibitor compounds. As a whole our results suggest areas for future development of more potent and druglike CBG inhibitors. A key result is the identification of a tripeptide retaining CDK2A binding and inhibitory activity. Although weak in potency, this compound represents the first peptide starting point devoid of strongly cationic residues. This will be important in the development of cell-permeable CBG inhibitors.

## Experimental Section

### Peptide synthesis

Solid-phase peptide synthesis was carried out by generic procedures based on Fmoc protection strategy chemistry[26] using an ABI 433A peptide synthesiser (Applied Biosystems, UK). All peptides were assembled in the form of C-terminal amides using Rink amide resins from Novabiochem (Merck Biosciences, UK). All other peptide synthesis reagents were obtained from ABI. Fmoc-protected amino acid derivatives were purchased from ABI or Peptech (US). After assembly, the peptides were cleaved from the resin using $i$Pr$_3$SiH/H$_2$O/CF$_3$CO$_2$H (5:5:90). The cleaved peptide solutions were diluted with H$_2$O and evaporated. RP-HPLC was performed using Vydac 218TP C$_{18}$ columns (analytical, 4.6×250 mm; preparative, 25×250 mm) with MeCN/0.1% aq CF$_3$CO$_2$H gradient elution. Mass spectrometry was performed using a Waters ZQ-2000 LC–MS system. Analytical details of the peptides synthesised is summarised in Table 4.

***N*$^{\alpha}$-Fmoc-α-hydroxy-β-homo**Leu **[(2*R*/*S*,3*S*)-3-amino-2-hydroxy-5-methylhexanoic acid]**: *Z*-L-Leucine (5.0 g, 18.8 mmol), *N*,*O*-dimethylhydroxylamine hydrochloride (2.2 g, 22.6 mmol) and 1-ethyl-3-(3′-dimethyl-aminopropyl)carbodiimide hydrochloride (WSC; 3.96 g, 20.7 mmol) were dissolved in CH$_2$Cl$_2$ (94 mL) and $i$Pr$_2$NEt (3.93 mL, 22.6 mmol) was added. The mixture was stirred for 2 h and was then evaporated. The residue was suspended in EtOAc (100 mL) and washed with aq HCl (50 mL, 2 M), saturated aq NaHCO$_3$ solution (50 mL), and brine (50 mL). After drying (Na$_2$SO$_4$), the organic phase was passed through a plug of silica gel to afford *Z*-L-Leucine *N*,*O*-dimethylhydroxylamide (3.87 g, 12.5 mmol), which was used in the next step without further purification. To a solution of this material in THF (93 mL) was added LiAlH$_4$ (25 mL, 1 M in Et$_2$O) and the mixture was stirred for 10 min. The reaction was then quenched by the addition of the minimum amount of saturated aq citric acid solution. The resulting solids were filtered and washed with EtOAc. The combined filtrates were dried and evaporated. The residue was redissolved in CH$_2$Cl$_2$ (62.5 mL) and cooled to −40°C, then treated with tributyltin cyanide (4.74 g, 15.0 mmol). The mixture was stirred at −40°C for 30 min, evaporated, resuspended in aq HCl/dioxane (62 mL, 6 M), and heated under reflux for 12 h. After cooling, dioxane was removed in vacuo and the aqueous phase was washed with Et$_2$O, adjusted to pH 5, and diluted with Me$_2$CO. This mixture was kept at −24°C for 72 h, and the product of (2*R*/*S*,3*S*)-3-amino-2-hydroxy-5-methylhexanoic acid collected by filtration. This material (~10 mmol) was dried and suspended in dioxane (20 mL). Saturated aq NaHCO$_3$ solution (10 mL) and Fmoc *N*-hydroxysuccinimide ester (3.37 g, 10 mmol) were added and the mixture was stirred overnight. EtOAc (50 mL) was added and the phases separated. The organic phase was washed with aq HCl (2 M) and brine, dried (Na$_2$SO$_4$), filtered, and evaporated. The residue was purified by column chromatography (silica gel, 10% MeOH in CH$_2$Cl$_2$), affording the title compounds as a diastereomeric mixture (~1:1 by anal. RP-HPLC; $t_R$ = 15.03 min & 17.35 min, linear gradient of 20–70% MeCN in 0.1% aq CF$_3$COOH over 20 min, 1 mL min$^{-1}$). Yield: 0.57 g, 12% with respect to *Z*-L-Leucine; $^1$H NMR (500 MHz, CDCl$_3$): $\delta$ 0.85 (m, 6H, 2C*H*$_3$), 1.25–1.75 (m, 3H, Me$_2$C*H*C*H*$_2$), 3.63 (m, 1H, C$^{\alpha}$*H*), 3.78 (m, 1H, C$^{\beta}$*H*), 4.04–4.38 (m, 2H, C*H*$_2$O), 4.42 (m, 1H, C*H*CH$_2$O), 7.20–7.80 (m, 8H, Ar*H*); MS (EI, − mode): *m/z* (%): 382.19 (100%) [*M*−H]$^-$, 381.93 (79%), 383.04 (5%); C$_{22}$H$_{25}$NO$_5$ = 383.17; Analytical data were consistent with literature reported values.[27]

### Biochemical assays

#### *Competitive binding assay*[14,16,17]

Using half-area black 96-well microtitre plates, 10 μL test compound solution (in 10% aq DMSO), 10 μL assay buffer (25 mM HEPES, pH 7, 10 mM NaCl, 0.01% Nonidet P-40, 1 mM dithiothreitol), 10 μL CDK2A (~0.3 μg/well purified recombinant human complex) in assay buffer, and 37.5 nM fluoresceinyl-AhxHisAlaLysArgArgLeullePhe-NH$_2$ tracer peptide in assay buffer was added to each well. After incubation with shaking for 1 h at room temperature, fluorescence polarisation was read on a Tecan Ultra plate reader fitted with 485 nm/535 nm excitation/emission filters and a dichroic mirror suitable for fluorescein. IC$_{50}$ values were determined

  

**Table 4.** Analytical data for peptides **1**–**23**.

| No. | Sequence | anal. RP-HPLC[a] | | | ESI-MS[e] | |
|---|---|---|---|---|---|---|
| | | $t_R$ (min)[b] | Gradient (MeCN, %)[c] | Purity (%)[d] | $M_r$ | *m/z* |
| **1** | H-HisAlaLysArgArgLeu**l**lePhe-$NH_2$ | 17.06 | 13-23 | >98 | 1039.3 | 1040.9 |
| **2** | H-AlaAlaAbuArgArgLeu**l**le*p*FPhe-$NH_2$ | 18.45 | 13-23 | >98 | 948.1 | 950.0 |
| **3** | H-AlaAlaAbuArgArgLeuPhe-$NH_2$ | 19.52 | 13-23 | >98 | 817.0 | 817.8 |
| **4** | H-AlaAlaAbuArgArgβhLeuPhe-$NH_2$ | 15.37 | 13-23 | 95 | 831.0 | 831.8 |
| **5** | H-AlaAlaAbuArgArgLeuαhPhe-$NH_2$ | 14.95 | 10-20 | 97 | 831.0 | 832.2 |
| **6** | H-AlaAlaAbuArgArgβhLeuαhPhe-$NH_2$ | 13.68 | 5-15 | >98 | 845.0 | 846.1 |
| **7** | H-AlaAlaAbuβhArgβhLeuPhe-$NH_2$ | 14.71 | 15-25 | 98 | 688.9 | 689.0 |
| **8** | H-ArgArgLeu**l**lePhe-$NH_2$ | 13.35 | 15-25 | >98 | 702.9 | 704.7 |
| **9** | H-ArgArgβhLeuPhe-$NH_2$ | 13.43 | 0-60 | 80 | 603.8 | 604.5 |
| **10** | Ac-ArgArgLeu**l**lePhe-$NH_2$ | 14.76 | 17-27 | >98 | 744.9 | 745.5 |
| **11** | Ac-ArgArgβhLeuPhe-$NH_2$ | 13.50 | 15-25 | >98 | 645.8 | 646.7 |
| **12** | Ac-ArgArgβhLeuMePhe-$NH_2$ | 18.38 | 15-25 | >98 | 675.8 | 676.6 |
| **13** | H-ArgArgLeuAsn*p*FPhe-$NH_2$ | 13.13 | 12-22 | >98 | 721.8 | 722.7 |
| **14** | H-ArgArgβhLeu*p*FPhe-$NH_2$ | 17.91 | 10-20 | >98 | 621.6 | 622.0 |
| **15** | H-ArgArgβhLeu*m*FPhe-$NH_2$ | 14.08 | 12-22 | >98 | 621.6 | 622.8 |
| **16** | H-ArgArgβhLeu*m*ClPhe-$NH_2$ | 17.23 | 12-22 | >98 | 638.2 | 638.5 |
| **17** | Ac-ArgArgLeuAsn*p*FPhe-$NH_2$ | 11.58 | 14-24 | >98 | 763.9 | 764.7 |
| **18** | Ac-LeuAsn*p*FPhe-$NH_2$ | 18.19 | 15-25 | >98 | 451.5 | 452.2 |
| **19** | Ac-βhLeu*p*FPhe-$NH_2$ | 14.35 | 0-60 | 70 | 351.4 | 350.4[f] |
| **20** | H-ArgArg-αOHβhLeu*p*FPhe-$NH_2$ | 16.10 | 15-25 | 80 | 637.8 | 638.3 |
| **21** | H-ArgArg-αOHβhLeu*p*FPhe-$NH_2$ | 19.80 | 15-25 | >98 | 637.8 | 638.2 |
| **22** | H-CitCitαOHβhLeu*p*FPhe-$NH_2$ | 16.40 | 15-25 | >95 | 639.7 | 640.1 |
| **23** | H-CitCitαOHβhLeu*p*FPhe-$NH_2$ | 21.30 | 15.25 | >98 | 639.7 | 640.2 |

[a] Refer Experimental Section. [b] $t_R$, retention time; [c] linear gradient of MeCN in 0.1% aq $CF_3CO_2H$ over 20 min; [d] by $A_{214\ nm}$ peak integration; [e] *m/z* values for the molecular ion $[M+H]^+$ are given; [f] $[M-H]^-$.

with the ActivityBase suite of software (IDBS, UK) using an unconstrained four-parameter dose-response equation.

**Keywords:** peptidomimetics · structure-based drug design · cyclin groove inhibitors · cyclin-dependent kinases · cancer

### *Functional kinase assay*[14, 16, 17]

Test compounds were added to reactions containing 50 mM HEPES, pH 7.4, 20 mM β-glycerophosphate, 5 mM EGTA, 2 mM dithiothreitol, 1 mM $NaVO_3$, and 20 mM $MgCl_2$, GST-pRb(773–928) solution, 2–5 μg of purified recombinant human CDK2A, 15 mM $MgCl_2$, and 100 μM ATP, spiked with 30–50 kBq per well of [γ-$^{32}$P]-ATP. Reactions were incubated with shaking for 30 min at 30 °C, before placing on ice, followed by addition of 5 μL/well of glutathione-Sepharose 4B (Amersham Biosciences, UK). Beads were allowed to bind for 30 min at room temperature with shaking, before filtering on Whatman GF/C filter plates. Plates were washed four times with 0.2 mL/well of 50 mM HEPES containing 1 mM ATP. Incorporated radioactivity was determined after adding 50 μL/well MicroScint40 (Packard) using a TopCount scintillation counter (Packard Instruments, UK). $IC_{50}$ values were determined with the ActivityBase suite of software (IDBS, UK) using an unconstrained four-parameter dose-response equation.

### X-ray crystallography and structure determination

For the purposes of crystallisation, human recombinant CDK2 and cyclin A2 (fragment encompassing residues 173–432) were produced as described in the literature.[14, 28] Crystals of the CDK2A–peptide **11**, **12**, **18**, and **21** complexes were obtained as described previously for other CDK2A–peptide complexes.[14, 16, 17] Data were collected at the Daresbury (UK) and Grenoble (France) synchrotron facilities and were processed as described.[14, 16, 17] Crystallographic data are summarised in Table 3 (PDB: 2WFY, 2WEV, 2WHA and 2WHB).

[1] D. O. Morgan, *Nature* **1995**, *374*, 131–134.
[2] M. Xu, K. A. Sheppard, C. Y. Peng, A. S. Yee, H. Piwnica-Worms, *Mol. Cell. Biol.* **1994**, *14*, 8420–8431.
[3] Y.-N. P. Chen, S. K. Sharma, T. M. Ramsey, L. Jiang, M. S. Martin, K. Baker, P. D. Adams, K. W. Bair, W. G. Kaelin, *Proc. Natl. Acad. Sci. USA* **1999**, *96*, 4325–4329.
[4] N. Mendoza, S. Fong, J. Marsters, H. Koeppen, R. Schwall, D. Wickramasinghe, *Cancer Res.* **2003**, *63*, 1020–1024.
[5] W. G. Kaelin Jr. , *Cancer Biol. Ther.* **2003**, *2*, S34–40.
[6] P. M. Fischer, *Cell Cycle* **2004**, *3*, 742–746.
[7] P. M. Fischer in *Cancer Drug Design and Discovery* (Ed.: S. Neidle), Academic Press, New York, **2008**, pp. 253–283.
[8] C. McInnes, M. J. I. Andrews, D. I. Zheleva, D. P. Lane, P. M. Fischer, *Curr. Med. Chem. Anti-Cancer Agents* **2003**, *3*, 57–69.
[9] N. R. Brown, E. D. Lowe, E. Petri, V. Skamnaki, R. Antrobus, L. N. Johnson, *Cell Cycle* **2007**, *6*, 1350–1359.
[10] K. Y. Cheng, M. E. Noble, V. Skamnaki, N. R. Brown, E. D. Lowe, L. Kontogiannis, K. Shen, P. A. Cole, G. Siligardi, L. N. Johnson, *J. Biol. Chem.* **2006**, *281*, 23167–23179.
[11] A. A. Russo, P. D. Jeffrey, A. K. Patten, J. Massague, N. P. Pavletich, *Nature* **1996**, *382*, 325–331.
[12] N. R. Brown, M. E. Noble, J. A. Endicott, L. N. Johnson, *Nat. Cell Biol.* **1999**, *1*, 438–443.
[13] E. D. Lowe, I. Tews, K. Y. Cheng, N. R. Brown, S. Gul, M. E. M. Noble, S. J. Gamblin, L. N. Johnson, *Biochemistry* **2002**, *41*, 15625–15634.
[14] G. Kontopidis, M. J. I. Andrews, C. McInnes, A. Cowan, H. Powers, L. Innes, A. Plater, G. Griffiths, D. Paterson, D. I. Zheleva, D. P. Lane, S. Green, M. D. Walkinshaw, P. M. Fischer, *Structure* **2003**, *11*, 1537–1546.
[15] P. D. Jeffrey, A. A. Russo, K. Polyak, E. Gibbs, J. Hurwitz, J. Massague, N. P. Pavletich, *Nature* **1995**, *376*, 313–320.
[16] M. J. I. Andrews, G. Kontopidis, C. McInnes, A. Plater, L. Innes, A. Cowan, P. Jewsbury, P. M. Fischer, *ChemBioChem* **2006**, *7*, 1909–1915.

  

[17] M. J. I. Andrews, C. McInnes, G. Kontopidis, L. Innes, A. Cowan, A. Plater, P. M. Fischer, *Org. Biomol. Chem.* **2004**, *2*, 2735–2741.
[18] G. Castanedo, K. Clark, S. Wang, V. Tsui, M. Wong, J. Nicholas, D. Wickramasinghe, J. C. Marsters, D. Sutherlin, *Bioorg. Med. Chem. Lett.* **2006**, *16*, 1716–1720.
[19] G. E. Atkinson, A. Cowan, C. McInnes, D. I. Zheleva, P. M. Fischer, W. C. Chan, *Bioorg. Med. Chem. Lett.* **2002**, *12*, 2501–2505.
[20] P. M. Fischer, *Med. Res. Rev.* **2007**, *27*, 755–795.
[21] G. Kontopidis, C. McInnes, S. R. Pandalaneni, I. McNae, D. Gibson, M. Mezna, M. Thomas, G. Wood, S. Wang, M. D. Walkinshaw, P. M. Fischer, *Chem. Biol.* **2006**, *13*, 201–211.
[22] D. I. Zheleva, C. McInnes, A.-L. Gavine, N. Z. Zhelev, P. M. Fischer, D. P. Lane, *J. Peptide Res.* **2002**, *60*, 257–270.
[23] J.-A. Fehrentz, B. Castro, *Synthesis* **1983**, 676–678.
[24] R. Herranz, J. Castro-Pichel, T. Garcia-Lopez, *Synthesis* **1989**, 703–706.
[25] P. B. W. Ten Kortenaar, B. G. Van Dijk, J. M. Peeters, B. J. Raaben, P. J. H. M. Adams, G. I. Tesser, *Int. J. Pept. Protein Res.* **1986**, *27*, 398–400.
[26] W. C. Chan, P. D. White (Eds.), *Fmoc Solid Phase Peptide Synthesis: A Practical Approach*, Oxford University Press, Oxford, **2000**.
[27] R. A. Tromp, M. Van Der Hoeven, A. Amore, J. Brussee, M. Overhand, G. A. Van Der Marel, A. Van Der Gen, *Tetrahedron: Asymmetry* **2003**, *14*, 1645–1652.
[28] S. Y. Wu, I. McNae, G. Kontopidis, S. J. McClue, C. McInnes, K. J. Stewart, S. Wang, D. I. Zheleva, H. Marriage, D. P. Lane, P. Taylor, P. M. Fischer, M. D. Walkinshaw, *Structure* **2003**, *11*, 399–410.

Received: February 11, 2009
Revised: April 1, 2009
Published online on ■■ ■■, 2009

  

*G. Kontopidis, M. J. Andrews, C. McInnes, A. Plater, L. Innes, S. Renachowski, A. Cowan, P. M. Fischer**

■■ – ■■

**Truncation and Optimisation of Peptide Inhibitors of Cyclin-Dependent Kinase 2-Cyclin A Through Structure-Guided Design**

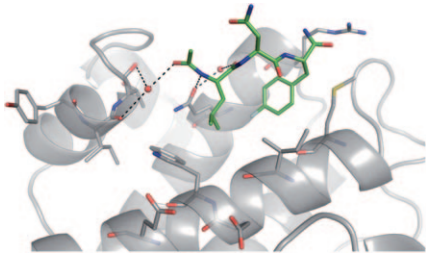

**Peptides that inhibit** cyclin-dependent kinase 2 by blocking the macromolecular substrate recruitment site of cyclin A were simplified, for example, by replacement of dipeptide units with β-amino acids. The smallest inhibitor retaining activity was a tripeptide, whose binding mode was confirmed by X-ray crystallography. This result suggests that non-peptidic cyclin groove inhibitors may be feasible therapeutic agents.

  